

Dear Editor,

We would like to thank you for your valuable contribution, which has significantly improved the quality and clarity of our manuscript. We have addressed all comments and provide detailed responses below:

1) Bu-NPP: In the abstract and conclusion, and to some extent in the main article, you don't mention the results from the Bu-NPP. You showed that the contribution is in fact the highest in springtime. You don't show any map of iodine or Cesium concentrations from the Bu-NPP in the paper. However, I assume the transport of radioactive materials pass over the northern part of Qatar and not the south. If the map is significantly different than the runs with B-NPP, you should add a map of the results showed on figure 10A and develop a little bit the results around Bu-NPP.

✓ **We have carefully considered your feedback and made the necessary revisions accordingly. In response to your suggestion, we have now incorporated a discussion and included maps pertaining to the emission from the Bushehr NPP in the abstract, conclusion, and relevant sections of the main article. Specifically, we have included a map in Figure 11, displaying iodine and Cesium concentrations from the Bu-NPP, thus providing a visual representation of the results.**

Lines 27-30:

“As part of a sensitivity analysis involving different model setups, changing the emission point from B-NPP to Bushehr-NPP (Bu-NPP) results in a reduced transfer of radioactive materials to Qatar, except in the spring season. Bu-NPP simulations reveal distinct spatial patterns, with peak ^{131}I concentrations and ^{137}Cs deposition observed in the northern and eastern Qatar during winter and spring.”

Lines 51-52:

“The Barakah Nuclear Power Plant (B-NPP) is the latest example, following the Bushehr NPP (Bu-NPP), to become operational in a region with unique climatological conditions.”

Lines 489-497:

“In Figure 11-A, a distinct spatial pattern emerges in the Bu-NPP simulations when compared to the B-NPP simulations (Figs. 5, 6, and 7). The simulated $^{131}\text{I}^{\text{intg_conc_full}}$ exhibit relatively high values in the northern and eastern regions, including Doha, particularly during the winter and spring seasons. This occurrence can be attributed to the downward movement of westerlies, facilitating the transport of air masses

enriched with ^{131}I towards these areas. The full-year median of the total ^{137}Cs deposition ($^{137}\text{Cs}^{\text{tot_depos_full}}$) (Fig. 11-B) closely follows this temporal pattern, showing prominent peaks during the spring and winter seasons within the northern and eastern regions of Qatar. Conversely, during the fall and summer seasons, the levels of $^{131}\text{I}^{\text{intg_conc_full}}$ and $^{137}\text{Cs}^{\text{tot_depos_full}}$ are greatly reduced. The age of particles corresponding to high levels of ^{131}I and ^{137}Cs simulations indicates their earlier entry into the northern half of Qatar during these two seasons, reaching the region within approximately 40-50 hours and 60 hours after release, respectively.”

Lines 506-509:

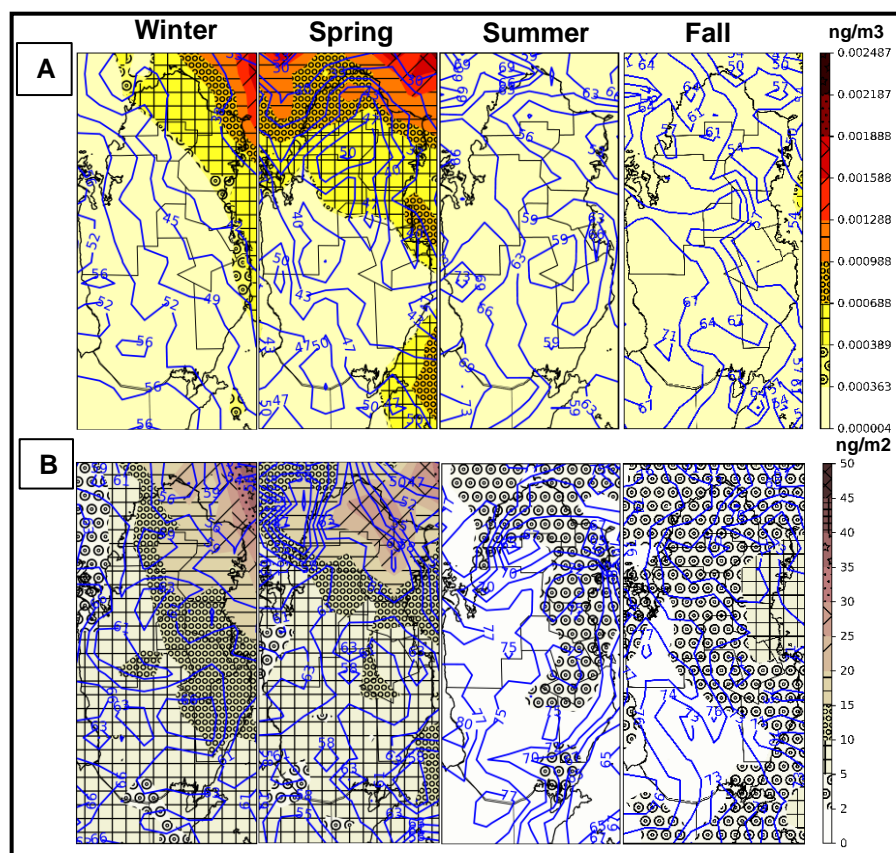


Figure 1: Simulated $^{131}\text{I}^{\text{intg_conc_full}}$ (A) and $^{137}\text{Cs}^{\text{tot_depos_full}}$ (B) based on ERA5-WRF inputs originating from Bushehr NPP. The contour lines are the full-year median of age spectra coinciding with the maximum ^{131}I concentrations and the completion of ^{137}Cs deposition found in each 96-hour run.

Lines 633-639:

“As anticipated, due to the longer distance, the change in the emission point from B-NPP to Bushehr-NPP (Bu-NPP) results in reduced transfer of radioactive materials to Qatar, except during the spring season. The simulations from Bu-NPP exhibit distinct spatial patterns compared to those from B-NPP. Concentrations of ^{131}I peak in the northern and eastern regions during winter and spring, which can be attributed

to a southward shift of the westerlies. The deposition of ^{137}Cs follows a similar pattern. The entry of particles inducing high intensities of ^{131}I and ^{137}Cs over the northern region of Qatar occurs within approximately 40-50 hours and 60 after their release, respectively.”

2) Line 50: You should also mention that the Bu-NPP is the second power plant in the MENA region.

✓ **Done. Lines 51-52** “The Barakah Nuclear Power Plant (B-NPP) is the latest example, following the Bushehr NPP (Bu-NPP), to become operational in a region with unique climatological conditions.”

3) Section 3.2: The results in section 3.2 would be more easily accessible if they were listed in a table.

✓ **After careful consideration, we have found that it is best to retain the current presentation style in Section 3.2 for conveying information regarding particle ages and their distribution. But, we have enhanced the presentation of results in subsection 3.1. While we have decided to retain the figures S2 and S3 showcasing scatter plots of the modeled and observed meteorological fields, we have also incorporated Table 3 specifically addressing the statistics of model performance against observations. We note that the table focuses on the statistics related to observations, and does not include model intercomparisons.**

Lines 289:

Table 3: Comparison of modelled and observed daily precipitation, wind speed, and temperature.

Variable	Mini-ensemble members	Spearman Correlation coefficient	RMSE	MBE
Precipitation (mm)	GFS	0.42	3.1	-0.18
	FNL	0.42	3	-0.18
	FNL-WRF	0.37	3.4	-0.27
	ERA5-WRF	0.44	3.3	-0.24
mean		0.41	3.2	-0.22
Wind Speed (m/s)	GFS	0.58	1.7	-0.13
	FNL	0.58	1.7	-0.15
	FNL-WRF	0.64	4.1	0.62
	ERA5-WRF	0.65	1.5	0.51
mean		0.61	2.2	0.21
Temperature (k)	GFS	0.97	2.1	0.02

	FNL	0.98	2	0.02
	FNL-WRF	0.98	1.8	0.07
	ERA5-WRF	0.97	2	-0.33
mean		0.975	1.975	-0.055

4) equation 3, line 116: either you explain each member of the equation, or you don't show it.

✓ **Done. We have addressed this by providing explanations for each member of the equation.**

Lines 112-118:

“The minimum value of time step Δt_i is 1 second. Δt_i is used only for the horizontal turbulent wind components of Equation 3.

$$\Delta t_i = \frac{1}{ctl} \min(\Delta \tau_{L_\omega}, \frac{h}{2\omega}, \frac{0.5}{\frac{\partial \sigma_\omega}{\partial z}}) \quad (3)$$

In Equation 3, h represents the height of the atmospheric boundary layer and z denotes the height of the model level. The constant ctl represents a predefined characteristic time scale. τ_{L_ω} is the Lagrangian timescale for the vertical velocity autocorrelation. Additionally, ω represents the turbulent vertical wind component, while σ_ω represents its standard deviation. To solve the Langevin equation for the vertical wind component, a shorter time step $\Delta t_\omega = \frac{\Delta t_i}{ifine}$ is used.”

5) Line 267-271: If you reach a resolution of 1km, you can for instance switch off a convective scheme that would be designed for coarser resolution because most of the deep convection will be resolved. So going to a finer scale might help in reducing the number of subgrid phenomena that need to be simulated.

✓ **In response to your suggestion, we have incorporated the following lines into the main manuscript:**

Lines 264-267:

"While this study did not specifically investigate model resolutions finer than 10 km, it is important to note that increasing the model resolution to 1 km or less provides the capability to resolve finer subgrid phenomena. This allows for the deactivation of convective schemes designed for coarser resolutions, as the resolved deep convection becomes more prominent."